at Bermuda, are associated with atmospheric transport from higher latitudes and altitudes. In the summer and autumn months the ozone levels remain uniformly low, even during the frequent periods of enhanced transport from Africa (D. Savoie, personal communication). Imposed on the relatively low day-to-day variability is a marked diurnal cycle which is easily seen in the hourly time series for March 1990 shown in the inset *b*. This diurnal cycle persists throughout the 3-year record and has an amplitude of ~2.5 p.p.b. with a maximum at ~08:00 local time (LT) and a minimum at ~17:00 LT (see inset *b*).

Both the diurnal and seasonal patterns at Barbados bear a striking resemblance to those seen at Samoa[9]. The seasonal maxima are roughly twice their respective seasonal minima, and the diurnal amplitudes are 1.8–2.8 p.p.b.v. per day. Oltmans[9] has already suggested that the diurnal pattern at Samoa, which follows the diurnal change in solar flux, is driven by the net chemical destruction of ozone. Detailed chemical calculations for the tropical South Pacific by Liu *et al.*[10], using the low NO_x levels observed for that region[8], yield daily ozone net destruction rates of 1.0–2.4 p.p.b.v. per day. This range, which depends on the ozone concentration, agrees with diurnal amplitudes observed at both tropical locations. We infer that Barbados also has extremely low levels of NO_x and a resulting net photochemical destruction of ozone. Although Bermuda's higher synoptic variability (particularly during the large winter and spring transport events) greatly increases the statistical variance, a similar diurnal cycle of ~2 p.p.b.v. per day in the hourly means is observed. This, together with the seasonal cycle, suggests that the ozone chemistry at Bermuda is also dominated by photochemical destruction.

Although the diurnal and seasonal patterns are very similar, note that the monthly means at Barbados are 8–10 p.p.b.v. higher than those at Samoa. Two explanations have been offered for this interhemispheric difference, which is also observed over the eastern Atlantic[18,19] and the Pacific[5]: either there is more effective downward transport of stratospheric ozone in the Northern Hemisphere[11,25], or there is chemical production of tropospheric ozone there, due to a higher background level of NO_x (ref. 26). Although our observations support the dominant role of transport, they may not be representative of the tropospheric column. For example, satellite measurements of tropospheric ozone[27] show a summertime maximum over Bermuda, whereas we find a minimum in the atmospheric boundary layer. Indeed, differences in both tropospheric ozone transport[11,17] and chemistry[1,28] may cause the seasonal cycle in ozone to vary with altitude. *In situ* systematic measurements of NO_x and ozone vertical profiles to determine the relative contributions of transport and chemistry over the North Atlantic are needed to resolve this question. □

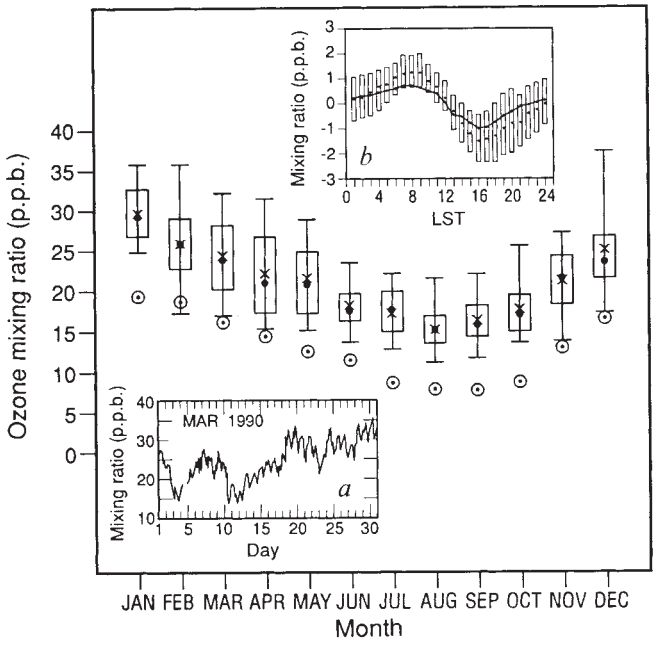

FIG. 3 Average monthly near-surface ozone mixing ratios at Barbados during the period April 1989–September 1991. Symbols are as in Fig. 1. The open circles are monthly median mixing ratios at American Samoa (1973–1991) offset by 6 months. Inset *a* shows the hourly mixing ratios at Barbados for March 1990. Inset *b* shows the average hourly deviations from the daily mean ozone mixing ratio at Barbados (1989–1991). The symbols are as in Fig. 1. The plus signs (+), which are connected by a solid line, are the hourly deviations at Samoa.

Received 6 January; accepted 5 June 1992.

1. Logan, J. A. *J. geophys. Res.* **90,** 10463–10482 (1985).
2. Liu, S. C. *et al. J. geophys. Res.* **92,** 4191–4207 (1987).
3. Isaksen, I. S. A., Jonson, J. F., Reeves, C. E., Solberg, S. & Chatfield, R. B. in *Ozone in the Atmosphere* (eds Bojkov, R. D. & Fabian, P.) 544–547 (Deepak, Hampton, 1989).
4. Fishman, J., Watson, C., Larsen, J. & Logan, J. *J. geophys. Rev.* **95,** 3599–3617 (1990).
5. Oltmans, S. J., Komhyr, W. D., Franchois, P. R. & Matthews, W. A. in *Ozone in the Atmosphere* (eds Bojkov, R. D. & Fabian, P.) 539–543 (Deepak, Hampton, 1989).
6. Logan, J. A. *J. geophys. Res.* **90,** 8511–8532 (1989).
7. Prospero, J. M. & Savoie, D. L. *Nature* **339,** 687–689 (1989).
8. McFarland, M. D., Kley, D., Drummond, J. W., Schmeltekopf, A. L. & Winkler, R. H. *Geophys. Res. Lett.* **6,** 605–608 (1979).
9. Oltmans, S. J. *J. geophys. Res.* **86,** 1174–1180 (1981).
10. Liu, S. C., McFarland, M., Kley, D., Zafiriou, O. & Huebert, B., *J. geophys. Res.* **88,** 1360–1368 (1983).
11. Levy II, H., Mahlman, J. D., Moxim, W. J. & Liu, S. C. *J. geophys. Res.* **90,** 3753–3772 (1985).
12. Crutzen, P. J. in *Tropospheric Ozone* (ed Isaksen, I. S. A. 3–32 (Reidel, New York, 1989).
13. Ramanathan, V., Cicerone, R. J., Singh, H. B. & Kiehl, J. T. *J. geophys. Res.* **90,** 5547–5566 (1985).
14. Volz, A. & Kley, D. *Nature* **332,** 240–242 (1988).
15. Simmonds, P. G. & Derwent, R. G. *Atmos. Envir.* **25a,** 1795–1808 (1991).
16. Schmitt, R., Schreiber, B. & Levin, I. *J. atmos. Chem.* **7,** 335–351 (1988).
17. Chatfield, R. & Harrison, H. *J. geophys. Res.* **82,** 5969–5976 (1977).
18. Winkler, P. *J. atmos. Chem.* **7,** 73–91 (1988).
19. Smit, H. G. J., Kley, D., McKeen, S., Volz, A. & Gilge, S. in *Ozone in the Atmosphere* (eds Bojkov, R. D. & Fabian, P.) 419–422 (Deepak, Hampton, 1989).
20. Oltmans, S. J. & Komhyr, W. D. *J. geophys. Res.* **91,** 5229–5236 (1986).
21. Levy II, H. *Nature* **325,** 761–762 (1987).
22. Danielsen, E. F. *J. atmos. Sci.* **25,** 502–518 (1968).
23. Merrill, J. T., Uematsu, M. & Bleck, R. *J. geophys. Res.* **94,** 8584–8598 (1989).
24. Browell, E. V., Danielsen, E. F., Ismail, S., Gregory, G. L. & Beck, S. M. *J. geophys. Res.* **92,** 2112–2120 (1987).
25. Mahlman, J. D., Levy II, H. & Moxim, W. J. *J. atmos. Sci.* **37,** 655–685 (1980).
26. Fishman, J. & Crutzen, P. J. *Nature* **274,** 855–858 (1978).
27. Fishman, J., Fakhruzzaman, K., Cross, B. & Nganga, D. *Science* **252,** 1693–1696 (1991).
28. Pittock, A. B. *Q. Jl R. met. Soc.* **103,** 575–584 (1977).

ACKNOWLEDGEMENTS. We thank S. Manabe for helpful comments. The trajectory calculations were performed by J. Merrill and the ozone observations by A. Glasspool and C. Shea.

Cirrus-cloud thermostat for tropical sea surface temperatures tested using satellite data

Rong Fu*, Anthony D. Del Genio†, William B. Rossow† & W. Timothy Liu‡

* Department of Atmospheric Sciences, University of California, Los Angeles, California 90024, USA
† NASA/Goddard Institute for Space Studies, New York, New York 10025, USA
‡ NASA/Jet Propulsion Laboratory, Pasadena, California 91109, USA

RAMANATHAN and Collins[1] have suggested cirrus clouds associated with tropical convection might act as a 'thermostat' to limit tropical sea surface temperatures (SSTs) to less than 305 K by shielding the ocean from sunlight. Here we use satellite radiance data to test this hypothesis. We find that changes in the properties of cirrus clouds do not seem to be related to changes in SSTs. During the 1987 El Niño event, large-scale perturbations to the radiative effects of cirrus clouds were controlled by changes in large-scale atmospheric circulation rather than directly by SSTs. If they are averaged over the entire tropical Pacific, increases in surface evaporative cooling are stronger than decreases in solar

heating owing to cirrus cloud variations. Thus we conclude that there is no 'cirrus cloud thermostat' to tropical SSTs.

Ramanathan and Collins[1] expressed their hypothesis as follows: "as the tropical oceans warm, the rapid rise of G_a (the atmospheric greenhouse effect) with SST leads to an unstable feedback. The warming continues until the clouds become thick enough to shield the ocean from the solar radiation and arrest further warming." This hypothesis is based largely on a supposed local correlation between anomalies in cloud forcing obtained from the Earth Radiation Budget Experiment (ERBE) and underlying SST anomalies between El Niño and non-El Niño years. But the tropical atmosphere-ocean system is strongly coupled by dynamics: a perturbation at one location influences other regions of the tropics as well. This fact raises three questions. Is the large-scale behaviour of clouds different from their local behaviour? Does cirrus-cloud variability depend on the underlying SST variation or on large-scale circulation variations? What is the importance of cloud-radiative feedback relative to other processes (such as surface evaporation) in regulating tropical SST?

To address these questions, we have analysed International Satellite Cloud Climatology Project (ISCCP) B3 radiance data[2] for the period January 1984–August 1987 (which covers almost a full El Niño cycle), and have derived changes in cirrus cloud amount (A_c), visible reflectance (R_c) and effective temperature (T_c). We used a visible-infrared threshold method to separate cirrus anvil clouds from both low or middle level clouds and small-scale convective towers[3]. Variations in SST and surface wind divergence were obtained from the Climate Analysis Center SST data[4] and Florida State University surface wind data[5], respectively.

To estimate the influence of cirrus cloud variations on broadband solar and thermal infrared fluxes at the surface, from the narrowband ISCCP radiances, we examined changes in a cloud solar index $\delta I_s = \delta[A_c(R_s - R_c)S_0]$ and in a cloud infrared index $\delta I_i = \delta[A_c\sigma(\mathrm{SST}^4 - T_c^4)]$ caused by changes in A_c, R_c and T_c (all obtained from the ISCCP data set). $S_0 = 339.5\ \mathrm{W\,m^{-2}}$ is the global annual mean incident solar flux at the top of the atmosphere, $\sigma = 5.67 \times 10^{-8}\ \mathrm{W\,m^{-2}\,K^{-4}}$ is Boltzmann's constant and $R_s = 6\%$ is the ocean surface reflectance.

We focus on changes in our solar index, which is defined as the difference between reflected visible radiance at the surface under clear conditions and that in the presence of cirrus (high-level) clouds. Our index isolates cases in which high-level clouds are present by excluding scenes dominated by lower-level clouds (ones which are warmer than the 500 mbar temperature). In contrast, the broadband ERBE index defined by Ramanathan and Collins[1] compares clear conditions with total fluxes that include the effects of other cloud types besides cirrus. The correlation between δI_s and ERBE shortwave cloud forcing anomalies for April 1987 minus April 1985 is 0.67 (for our sample size, a 0.12 correlation is significant at the 99% level of confidence, so the probability is $\ll 1\%$ that the correlation of 0.67 occurs by chance), indicating the importance of other cloud types.

We include the infrared index for illustrative purposes only. This index is a measure of the difference between the brightness temperature (effective temperature, T_c) for scenes with high-level clouds, and the surface temperature in the absence of such clouds. As for the solar index, the high-level cirrus clouds are isolated and the lower-level ones excluded. Thus, anomalies in this index represent changes in the greenhouse effect of cirrus clouds without including the effect of the atmosphere. The Ramanathan and Collins ERBE index contrasts broadband fluxes at the top of the atmosphere in cloudy and clear conditions; interannual anomalies in their index therefore include the effects of changes not only in cirrus but also in water vapour and other cloud types. For April 1987 minus April 1985, the correlation between δI_i and ERBE longwave cloud forcing anomalies is 0.62. Note, though, that neither ERBE longwave cloud forcing nor our index represents the effect of clouds on surface fluxes, which are dominated by emission from water vapour and low-level clouds[6].

We have correlated monthly δI_s with δI_i and δR_c with δT_c on three spatial scales: 2.5° latitude-longitude grid boxes (the scale considered in ref. 1), the tropical west (124° E–172° W, 25° S–25° N) and east (172° W–90° W, 25° S–25° N) Pacific (which averages over the Hadley circulation but separates the upwelling and downwelling branches of the Walker circulation), and the entire tropical Pacific (124° E–90° W, 25° S–25° N). Figure 1 shows the correlations of δI_s against δI_i and of δR_c against δT_c for 2.5° grids in the tropical Pacific for April 1987 minus April 1985 (an El Niño month minus a non-El Niño month, Fig. 1*a* and *c*), and for April 1984 minus April 1985 (two non-El Niño months, Fig. 1*b* and *d*). Figure 1*a* is analogous to Fig. 3*b* of ref. 1 except for the broader latitudinal range which does not affect the result.

The negative correlation between δI_s and δI_i means that a local increase in greenhouse effect is associated with a decrease in incoming solar radiation, which is consistent with ref. 1. Figure 1*c* shows that this negative correlation occurs at least in part because brightening of cirrus is associated with colder cirrus

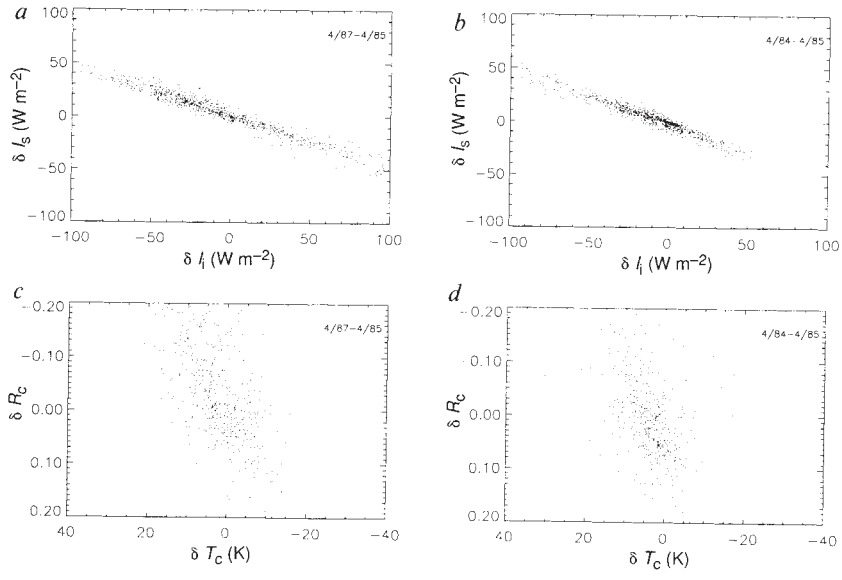

FIG. 1 *a*, Scatter plot of solar against infrared flux-index differences for cirrus clouds (δI_s and δI_i, respectively, in W m^{-2}) for April 1987 minus April 1985. These are for individual 2.5° × 2.5° latitude–longitude grid boxes in the tropical Pacific. The flux indices are defined to be positive downward. *b*, As in *a* but for April 1984 minus April 1985. *c*, As in *a* but for cirrus-cloud visible reflectance differences (δR_c, dimensionless) against cirrus-cloud infrared brightness temperature differences (δT_c, in kelvin). *d*, As in *c* but for April 1984 minus April 1985.

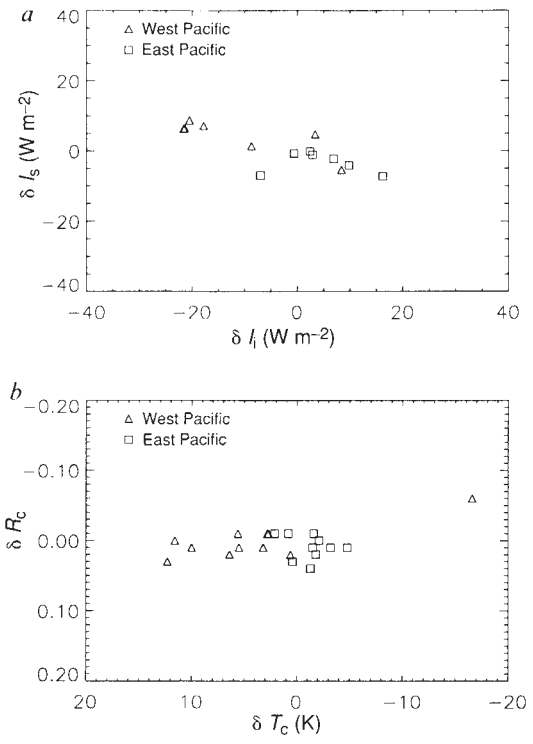

FIG. 2 *a*, Scatter plot of large-scale monthly mean I_s anomalies (δI_s) against I_i anomalies (δI_i) for 1987 minus 1985. The triangles represent anomalies averaged over the tropical west Pacific for each available month. The squares are defined similarly for data averaged over the tropical east Pacific. *b*, As in *a* but for cirrus-cloud visible reflectance anomalies (δR_c) against cirrus-cloud infrared brightness temperature anomalies (δT_c).

radiating temperatures (owing to higher cloud tops except for the thinner clouds), as assumed in ref. 1. Ramanathan and Collins interpret this correlation as meaning that the greenhouse effect "increases significantly with a warming of the ocean, and this unstable increase is effectively offset by the brighter clouds resulting from the warming."[1] But Fig. 1*b* and *d* shows that similar negative correlations occur even when the two non-El Niño months with minimal SST differences are compared. Thus, the relationship that forms the basis of the proposed thermostat mechanism is observed even when SST does not change, indicating that the cloud anomalies do not result from SST anomalies.

We repeated the analysis of Fig. 1*a* and *c*, but with data averaged over either the west or east Pacific (Fig. 2), to remove mesoscale variations, account for compensating effects within the Hadley cell and focus on differences between the rising and sinking branches of the Walker circulation. The negative correlation between large-scale δI_s and δI_i is less apparent (Fig. 2*a*). Incoming solar radiation slightly decreased or did not change in the east Pacific while increasing slightly or remaining constant in the west Pacific during the 1987 El Niño. Similarly, longwave-radiation trapping generally increased in the east Pacific and decreased in the west Pacific. Figure 2*b* shows that the changes in radiative indices were neither associated with any systematic anomaly in cirrus-cloud reflectance in either region nor with any cloud-top temperature anomaly in the east Pacific (where a longwave trapping anomaly is nevertheless present). Thus, El Niño perturbations of cloud radiative effects occur mainly through changes in cloud cover, not cloud top height or optical thickness. When we averaged the results over the entire tropical Pacific (not shown), we found no systematic changes caused by cirrus ($\delta I_s = -0.9$, $\delta I_i = -1.2$ W m^{-2}), even though the basin-wide SST was warmer during the El Niño. This is because El Niño cloud changes are dominated by the geographic relocation of cirrus associated with moist convection, so that radiative variations in one area are compensated by opposite changes elsewhere.

To determine the relative impact of SST and dynamics on cirrus variability, we correlated large-scale δI_s for individual months from 1984 and 1987 with SST and surface wind divergence anomalies (Fig. 3). δI_s correlates with SST changes only in the east Pacific (Fig. 3*b*): less solar radiance is absorbed in the warmer year. In the west (Fig. 3*a*), opposite but equally large solar anomalies occur despite the absence of any SST anomaly. In both west (Fig. 3*c*) and east (Fig. 3*d*) Pacific, enhanced surface convergence occurs in the rising branch of the Hadley cell in the El Ninõ year. In the west, this is accompanied by an increase in incoming solar flux, whereas in the east incoming solar flux decreases.

As SST and divergence anomalies are themselves correlated in the east Pacific, it is difficult to separate their individual effects

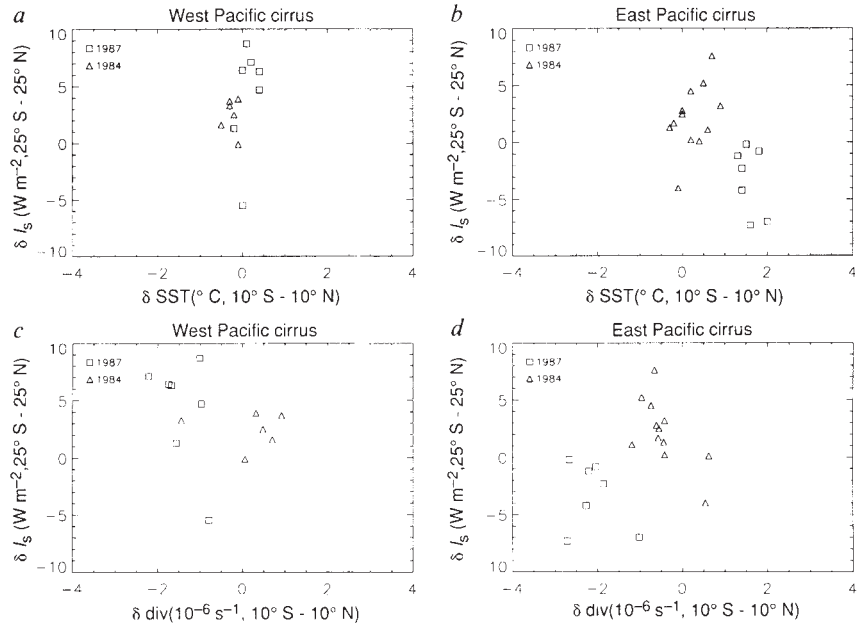

FIG. 3 *a*, Scatter plot of large-scale monthly mean cirrus solar flux-index anomalies averaged over latitudes 25° S–25° N (δI_s) against SST anomalies (δSST) averaged over latitudes 10° S–10° N for two different years relative to 1985 in the west Pacific. The squares represent 1987 minus 1985 anomalies for each available month; the triangles are defined similarly for 1984 minus 1985. *b*, As in *a* but for the east Pacific. *c*, As in *a* but for solar flux-index anomalies against surface wind divergence anomalies (δdiv), with δdiv averaged over 10° S–10° N. *d*, As in *c* but for the east Pacific.

on cirrus. But it is clear that there is no compelling evidence for an intrinsic and local relationship between SST and large-scale cirrus anvil properties in the tropics. This is especially true in the west Pacific region of maximum SSTs, where solar radiation changes as large as those in the east occur without any SST variation. In the absence of a correlation between west Pacific cloud and SST variations, SST cannot be limited to 305 K by feedbacks with cirrus clouds, as is asserted in ref. 1. We conclude that there is no evidence for the thermostat mechanism on climatically significant spatial and temporal scales.

SST is determined by a balance between ocean heat-transports and surface energy fluxes. In the tropical oceans, solar irradiance and evaporation are the dominant variable components of the surface heat flux on both monthly and interannual timescales. Ramanathan and Collins discount evaporation as a limiting factor for SST[1]. To estimate the significance of latent heat flux anomalies, latent heat fluxes averaged over the entire tropical Pacific for January–August in both 1985 and 1987 were computed using a bulk parameterization model which accounts for atmospheric stability and the transition from rough air flow (moderate winds) to smooth air flow (low winds)[7]. Input parameters include SST from the Climate Analysis Center and surface wind speeds from Florida State University. The sea–air temperature difference and relative humidity are assumed to be 0.5 °C and 80%, respectively. The average evaporative flux during 1987 is 11.5 W m^{-2} stronger than that for 1985. The difference is significantly larger than δI_s (-0.9 W m^{-2}) indicating that evaporation is important for the interannual variation of surface heat flux.

Satellite observations for the 1982–1983 El Niño demonstrate that there is no significant correlation between local anomalies in surface solar irradiance and anomalous changes in SST[8]. But over a broad region south of the Equator (corresponding to large SST anomalies), there is a significant correlation between anomalous increase (decrease) in evaporation and anomalous decrease (increase) in SST. The opposite is true north of the Equator. Based on the arguments presented here, we see no evidence for the conclusion that cirrus clouds are the primary regulator of tropical SSTs. □

Received 24 January; accepted 15 June 1992.

1. Ramanathan, V. & Collins, W. *Nature* **351,** 27–32 (1991).
2. Schiffer, R. A. & Rossow, W. B. *Bull. Am. met. Soc.* **66,** 1498–1505 (1985).
3. Fu, R., Del Genio, A. D. & Rossow, W. B. *J. Climat.* **3,** 1129–1152 (1990).
4. Reynolds, W. B. *J. Clim. appl. Met.* **22,** 447–458 (1983).
5. Goldenberg, S. B. & O'Brien, J. J. *Mon. Weath. Rev.* **109,** 1190–1206 (1981).
6. Fung, I. Y., Harrison, D. E. & Lacis, A. A. *Rev. Geophys. Space Phys.* **22,** 177–193 (1984).
7. Liu, W. T., Katsaros, K. B. & Businger, J. A. *J. atmos. Sci.* **36,** 1722–1735 (1979).
8. Liu, W. T. & Gautier, C. *J. geophys. Res.* **95,** 13209–13217 (1990).

ACKNOWLEDGEMENTS. We thank I. Fung, M. Cane, D. Neelin and M. Ghil for constructive discussions, Y. Zhang for providing ISCCP-derived radiative fluxes and W. Tang for providing surface latent heat fluxes. This work was supported by the DOE Quantitative Links Program, the International Satellite Cloud Climatology Project, and the NASA Earth Observing System Interdisciplinary Sciences Program at JPL.

Frequency variations of the Earth's obliquity and the 100-kyr ice-age cycles

Han-Shou Liu

NASA/Goddard Space Flight Center, Geodynamics Branch, Greenbelt, Maryland 20771, USA

VARIATIONS in the Earth's orbital parameters modulate the seasonal distribution of solar radiation and thereby induce changes in the Earth's climate[1]. Periodicities in the geological climate record with cycles of 100, 41 and 23 kyr have been linked with changes in eccentricity, obliquity and precession of the equinoxes, respectively[2,3]. But although the eccentricity does vary with a 100-kyr period, the effect on the incoming solar radiation is rather weak relative to the signals from obliquity and precession variations. The 100-kyr signal in the climate record should therefore be of negligible intensity, yet it is observed instead to dominate the record. Internal, nonlinear processes within the climate system have been proposed to account for this fact[4–14]. In contrast, I show here that variations in the frequency of the obliquity cycle can give rise to strong 100-kyr forcing of climate.

Variation of the orbital obliquity is governed by[2]

$$\varepsilon_{(t)} = \varepsilon + \sum_{i=1}^{N} A_i \cos(\omega_i t + \beta_i) \qquad (1)$$

where $\varepsilon_{(t)}$ is the obliquity, and A_i, ω_i and β_i are the amplitude, mean frequency and phase angle for each component, respectively. The initial value of ε is 23.320556° and time $t = 0$ refers to AD 1950. From astronomical solutions for variation in the Earth's orbital elements[2], the variations of the obliquity can be calculated from equation (1). The results are as follows. During the past 10^6 years, the obliquity has oscillated for 24.57 cycles with a mean period of $T_0 = 40.7$ kyr. Two groups of longer- and shorter-period oscillations with mean period of ~42.2 kyr and 38.9 kyr (below the normal mean T_0) have occurred intermittently. The maximum values of the obliquity occurred at −9, −49, −92, −132, −171, −213, −252, −296, −334, −374, −416, −457, −499, −538, −579, −621, −663, −702, −743, −785, −827, −869, −906, −949 and −989 kyr; and the minima at −29, −70, −112, −150, −192, −232, −274, −316, −353, −396, −436, −479, −518, −558, −600, −642, −683, −722, −764, −805, −849, −887, −927, −970 kyr. In the longer period of oscillations, the glacial phases are ~4 kyr longer than the deglacial phases. Finally, a special group of 12 obliquity oscillations has an asymmetry such that the part of the cycle that has higher tilt is shorter than the part that has lower tilt. Consequently, the period or frequency of the obliquity variation is not constant. This variation of obliquity frequency may have considerable dynamical implications because the longer glacial phases in the cycles with longer periods would produce larger ice-age ice sheets or glaciers. Most important, the special set of the 12 asymmetrical cycles, in which the deglacial phases are ~3.5 kyr shorter than the normal mean value of $T_0/2$, may accelerate the warmer summer seasons and cause rapid deglacial melting. Therefore, frequency variation in the Earth's obliquity may be an important link between the astronomical theory of climate changes and the 100-kyr glacial cycles.

The concept of the instantaneous frequency of planetary motions[15] is useful for understanding the dynamical behaviour of planetary rotation[16,17] and libration[18,19]. Inspired by the time-frequency idea for investigation of planetary motions, I have applied this method to analyse the Earth's obliquity data and discovered that the frequency variation of the obliquity has a period of 100 kyr. To analyse the effect of these frequency variations on climate changes, we can express equation (1) as[20,21]

$$\begin{aligned}\varepsilon_{(t)} - \varepsilon = \sum_{i=1}^{N} A_i \cos(\omega_i t + \beta_i) &= A_{(t)} \cos \Phi_{(t)} \\ &= A_{(t)} \cos[\omega_0 t + \phi_{(t)}] \\ &= A_{(t)} \cos \omega_{(t)} t \qquad (2)\end{aligned}$$

where $A_{(t)}$ is the amplitude, $\Phi_{(t)}$ is a phase function, $\phi_{(t)}$ is phase angle, $\omega_0 = 2\pi/T_0 = 0.1543783$ rad kyr^{-1} and $\omega_{(t)}$ is the instantaneous frequency. Equation (2) formulates the obliquity variation for angle modulation which can be analysed in terms of frequency modulation. This is a form of angle modulation in which the instantaneous radian frequency $\omega_{(t)}$ is equal to a